UniVVT: A Unified End-to-End Framework for High-Fidelity Video Virtual Try-on

Yushe Cao[*1] **Shikun Feng**[*†2], **Fei Shen**[3], **Haikuo Peng**[4], **Jianqiang Xia**[5],
Yiheng Zhu[2], **Dianxi Shi**[†1], **Chun Yu**[†1],

[1]Tsinghua University [2]Zhongguancun Academy [3]National University of Singapore
[4]National University of Defense Technology [5]Shanghai Jiao Tong University
cao-ys23@mails.tsinghua.edu.cn,kunayumi@163.com

arXiv:2608.05745v1 [cs.CV] 6 Aug 2026

Abstract

Video Virtual Try-On (VVT) synthesizes a video of a person wearing a target garment while preserving identity, motion, and scene dynamics. Dominant approaches cast VVT as mask-conditioned video inpainting and rely on separate modules for human parsing, pose estimation, and garment warping. This multi-stage design complicates deployment and, more critically, allows errors in explicit geometric priors to propagate irreversibly into the generated video. We present UniVVT, a unified end-to-end framework that reframes VVT as semantically conditioned video generation, eliminating mask, pose, and warping modules at inference. At its core, a scene-task perceiver built on a Multimodal Large Language Model jointly encodes the source video, target garment, and task instruction into compact, task-aware latent tokens, implicitly capturing what to transfer and where and how to transfer it. A lightweight semantic bridge then aligns these tokens with the conditioning space of a diffusion-based video generator, enabling coherent garment transfer. To robustly couple the heterogeneous components, we devise a three-stage progressive training strategy comprising semantic alignment, joint task adaptation, and flexible-resolution refinement. Extensive experiments demonstrate that UniVVT achieves state-of-the-art performance across multiple benchmarks, validating implicit semantic guidance as a simple and effective alternative to fragile geometric preprocessing for end-to-end virtual try-on.

1 Introduction

Video Virtual Try-On (VVT) synthesizes videos of a person wearing a target garment, enabling dynamic garment visualization for online retail, fashion content creation, and digital humans (Jiang et al. 2022; Zou et al. 2025; Zuo et al. 2025). Compared with image-based virtual try-on (Yang et al. 2020; Zhu et al. 2023; Morelli et al. 2023; Jiang et al. 2024), VVT must preserve fine-grained garment appearance in every frame while modeling temporally coherent person–garment interactions under motion, deformation, and occlusion. These coupled requirements for spatial fidelity and temporal consistency make VVT substantially more challenging than static try-on.

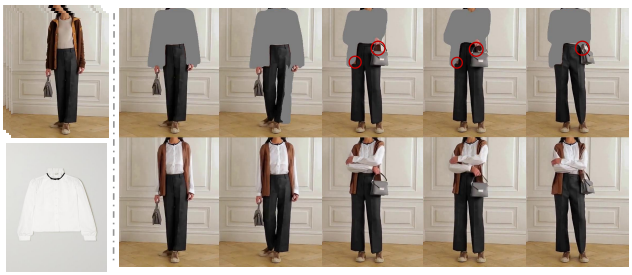


Figure 1: Failure cases caused by inaccurate masks. Leaked details from the original outerwear (top) contaminate the generated blouse (bottom), exposing the fragility of preprocessing-dependent VVT pipelines.

Most VVT methods inherit the image-based paradigm (Xu et al. 2025; Chong et al. 2024; Wang et al. 2025; Zhang et al. 2026): they cast try-on as temporal inpainting and use auxiliary models to extract clothing-agnostic masks, parsing maps, pose sequences, or DensePose representations before garment warping and synthesis (Fang et al. 2024b; Chong et al. 2025; Li et al. 2025). This multi-stage pipeline has three coupled limitations. First, errors from explicit geometric cues propagate to outputs and cause source residuals, incomplete garment replacement and boundary artifacts under occlusions or large motions (Figure 2). Second, many dedicated sub-models increase computational overhead and deployment complexity. Third, disjoint stage-wise optimization stops the generator from compensating upstream errors.

We propose UniVVT, a unified end-to-end framework that instead formulates VVT as semantically conditioned video generation. Our key insight is that *what* to transfer and *where* and *how* to transfer it can be encoded implicitly by multimodal semantics rather than prescribed through masks, poses, or warping fields. UniVVT realizes this idea through implicit guidance. A Multimodal Large Language Model (MLLM) (Bai et al. 2025) serves as a Scene-Task Perceiver, jointly encoding the source video, target garment, and task instruction into compact task-aware latent tokens. A lightweight Semantic Bridge projects these tokens into the conditioning space of a diffusion-based video generator. UniVVT thereby integrates task perception, semantic

[*]These authors contributed equally.
[†]Corresponding author.
This manuscript is a preprint and is currently under review for journal/conference publication.

alignment, and synthesis without external parsing, pose, or warping modules at inference. Additionally, we introduce a three-stage progressive training strategy to bridge representation gaps among heterogeneous components and stably train a high-fidelity try-on generator. Evaluations on benchmarks including ViViD-S (Fang et al. 2024b) verify UniVVT's competitive performance on both image and video virtual try-on. Removing fragile geometric preprocessing further simplifies deployment.

Our contributions are summarized as follows:

- We reformulate VVT as semantically conditioned video generation and propose UniVVT, a unified end-to-end framework that requires no external masks, pose estimation, or garment warping at inference.
- We introduce an implicit guidance mechanism comprising an MLLM-based Scene-Task Perceiver and a lightweight Semantic Bridge, which translate raw multimodal inputs into task-aware conditions for coherent try-on generation.
- We develop a three-stage progressive training strategy to stabilize adaptation across heterogeneous pretrained components. Comprehensive experiments on commonly used benchmarks validate the effectiveness and generality of the proposed framework.

2 Related Work

2.1 From Image to Video Virtual Try-On

Image-based virtual try-on has evolved from explicit warp-and-render pipelines (Yang et al. 2020; Minar et al. 2020; Ge et al. 2021) to diffusion-driven conditional generation (Morelli et al. 2023; Yang et al. 2024; Velioglu et al. 2024; Xing et al. 2025; Zhang et al. 2026). Early methods align garments with target bodies via geometric transformations or learned flow fields before feeding them into generative networks for final synthesis (Bookstein 2002; Han et al. 2019; Ge et al. 2021). Diffusion models greatly boost visual realism and garment fidelity (Zhu et al. 2023; Fang et al. 2024a; Song et al. 2025). Representative approaches including OOTDiffusion (Xu et al. 2025), IDM-VTON (Choi et al. 2024), StableVITON (Kim et al. 2024), and FitDit (Jiang et al. 2024) further strengthen garment conditioning via tailored attention modules and feature injection. Nevertheless, most existing methods rely heavily on explicit spatial priors such as parsing masks, human poses, and warped garments, making synthesis vulnerable to preprocessing errors.

Video virtual try-on inherits and exacerbates these limitations along the temporal dimension. Early pipelines perform frame-wise warping and rendering (Zhong et al. 2021; Dong et al. 2019), while ClothFormer (Jiang et al. 2022) captures cross-frame dependencies after garment deformation. Recent diffusion-based methods enhance temporal consistency using spatio-temporal attention (Fang et al. 2024b; Zou et al. 2025; Zheng et al. 2024), feature concatenation (Chong et al. 2025; Li et al. 2025), staged keyframe synthesis, motion-aware modeling, and positional encoding (Pan et al. 2025; Zuo et al. 2025). Despite progress, prevailing solutions remain formulated as preprocessing-dependent video inpainting (Blattmann et al. 2023; Karras et al. 2024): temporally consistent masks and poses predefine where and how edits are applied prior to generation. This causes upstream errors to propagate over frames, and disjointly optimized modules increase overall system complexity. UniVVT breaks this paradigm by replacing explicit geometric intermediates with task-aware semantic conditioning.

2.2 LLMs and MLLMs for Generative Guidance

Large Language Models (LLMs) and Multimodal Large Language Models (MLLMs) provide strong instruction understanding and multimodal reasoning capabilities (Qwen Team 2026; Bai et al. 2025; Singh et al. 2025; Deng et al. 2025; Comanici et al. 2025; Cheng et al. 2026). Existing image-editing systems use language models to construct editing instructions or translate user intent into conditions for diffusion models (Brooks, Holynski, and Efros 2023; Taseer 2024). In video generation, LLMs and MLLMs have primarily served as instruction refiners, storyboard planners, or high-level coordinators (Wang et al. 2024; Yuan, Chen, and Ng 2025; Zhao et al. 2025; Mou et al. 2025). Their latent representations, however, remain underexplored as direct conditioning signals for fine-grained, temporally structured editing. UniVVT employs the MLLM as a scene-task perceiver rather than a text generator: it jointly encodes the source video, target garment, and task instruction into compact latent tokens, which a lightweight semantic bridge maps to the conditioning space of a video diffusion model. This design turns multimodal understanding into implicit generative guidance and removes the need to specify the edit through masks, poses, or warping fields at inference.

3 Methodology

3.1 Problem Formulation and Overview

Given a source video $\mathbf{V}_{\text{in}}$, a target garment image $\mathbf{I}_{\text{gar}}$, and a textual instruction $\mathbf{T}_{\text{inst}}$, video virtual try-on aims to synthesize an output video $\mathbf{V}_{\text{out}}$ that dresses the person in the target garment while preserving the person's identity, original motion, scene context, and temporal coherence.

Unlike inpainting approaches that depend on preprocessing, UniVVT formulates VVT as a video generation task under implicit semantic guidance. Without using explicit masks, poses, or warped garments to prescribe the editing region, UniVVT derives a compact task-aware semantic representation from raw multimodal inputs. As illustrated in Figure 2, UniVVT comprises three components: (1) a multimodal **Scene-Task Perceiver** that encodes the try-on context, (2) a lightweight **Semantic Bridge** that maps the resulting representation into the generator's conditioning space, and (3) a **Video Generation Module** that synthesizes the final video through iterative denoising. By unifying task perception and video generation, UniVVT requires no external modules for explicit geometric encoding at inference.

3.2 Scene-Task Perceiver

The Scene-Task Perceiver transforms the source video, target garment, and textual instruction into a compact representation of the try-on objective. We instantiate it with the pretrained Qwen3-VL-2B-Instruct (Bai et al. 2025), denoted by

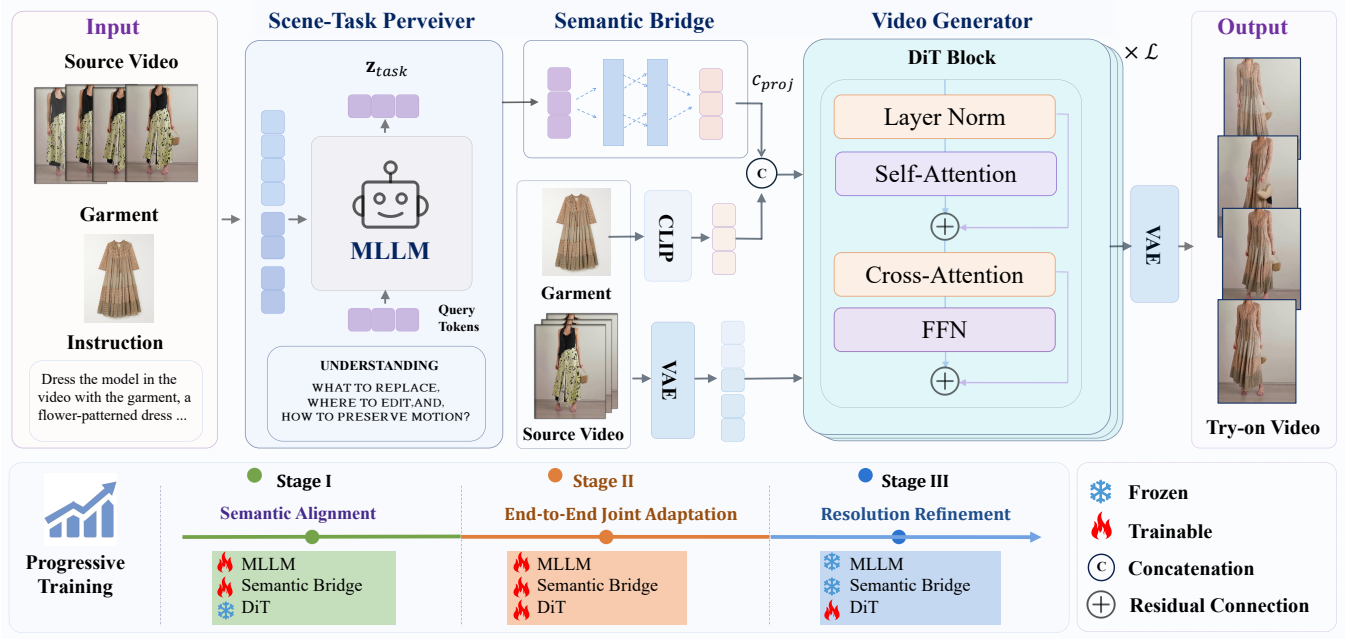


Figure 2: Overview of UniVVT. UniVVT consists of a scene-task perceiver that comprehensively understands the try-on task and extracts compact task-aware representations, which are then aligned to the conditional space of the generative model through a semantic bridge to implicitly guide virtual try-on video generation. A progressive training strategy further enables effective collaboration among components for better adaptation to the VVT task.

π_{mllm}, and use its hidden states as multimodal features rather than decoding text.

Input tokenization. We uniformly sample key frames from $\mathbf{V}_{\text{in}}$ and convert them into visual tokens using the MLLM's vision encoder. The garment image $\mathbf{I}_{\text{gar}}$ supplies the target appearance, while $\mathbf{T}_{\text{inst}}$ specifies the task. These inputs are organized into a unified token sequence following the native multimodal format of the MLLM.

Task-aware latent extraction. We prepend N learnable task queries $\mathbf{Q}_{\text{task}}$ to the multimodal sequence. Through self-attention, these queries aggregate task-relevant information across the instruction, video, and garment tokens. Their final hidden states define the task-aware latent representation

$$\mathbf{z}_{\text{task}} = \text{Extract}_{\mathbf{Q}}(\pi_{\text{mllm}}([\mathbf{Q}_{\text{task}}; \mathbf{T}_{\text{inst}}; \mathbf{V}_{\text{in}}; \mathbf{I}_{\text{gar}}]))\,. \quad (1)$$

Unlike masks or pose maps, $\mathbf{z}_{\text{task}}$ jointly captures garment attributes, scene context, body–garment correspondence, and temporal editing intent in a dense semantic representation. It therefore provides a task-specific interface between multimodal understanding and video generation without hand-crafted geometric supervision.

3.3 Semantic Bridge

The task latent $\mathbf{z}_{\text{task}}$ and the video generator occupy heterogeneous feature spaces, creating both dimensional and distributional mismatches. We therefore introduce a lightweight trainable Semantic Bridge $\mathcal{P}_\theta$ that projects $\mathbf{z}_{\text{task}}$ into generator-compatible conditioning tokens:

$$\mathbf{c}_{\text{proj}} = \mathcal{P}_\theta(\mathbf{z}_{\text{task}}), \qquad \mathbf{c}_{\text{proj}} \in \mathbb{R}^{N \times d_{\text{cond}}}. \quad (2)$$

Here, N is the number of task queries and d_{cond} is the generator's conditioning dimension. Implemented as a compact multi-layer perceptron, $\mathcal{P}_\theta$ serves as a semantic adapter rather than learning new generative priors. It translates high-level cues—*what* to transfer, *where* to edit, and *how* to maintain appearance over time—into conditioning signals that modulate the denoising process.

3.4 Video Generation Module

Our generator $\mathcal{G}_\phi$ builds on a pretrained latent video diffusion model with a Diffusion Transformer (DiT) backbone (Wang, Ai et al. 2025). It synthesizes a high-fidelity, temporally coherent try-on video through iterative denoising under joint structural, appearance, and semantic conditioning.

Latent input construction. A pretrained causal video VAE encodes $\mathbf{V}_{\text{in}}$ and $\mathbf{I}_{\text{gar}}$ into the source-video latent $\mathbf{z}_{\text{video}}$ and garment latent $\mathbf{z}_{\text{gar}}$. At each denoising step, we concatenate $\mathbf{z}_{\text{video}}$ with the noisy latent $\mathbf{x}_t$ along the channel dimension, retaining identity, motion, and background structure. We then append $\mathbf{z}_{\text{gar}}$ along the sequence dimension as a static appearance reference. The resulting latent sequence is denoted by $\mathbf{T}^{\text{in}}_{\text{seq}}$.

Condition injection. While $\mathbf{c}_{\text{proj}}$ specifies the desired edit, its compact representation may omit fine garment appearance. We therefore extract a complementary feature $\mathbf{f}_{\text{clip}}$ from $\mathbf{I}_{\text{gar}}$ using a frozen CLIP image encoder (Cherti et al. 2023). Each DiT block injects both conditions through cross-attention. Specifically, $\mathbf{T}^{\text{in}}_{\text{seq}}$ produces queries $\mathbf{Q}$, whereas the task and CLIP features produce concatenated keys $\mathbf{K}_c$ =

$[\mathbf{K}_{\text{task}}; \mathbf{K}_{\text{clip}}]$ and values $\mathbf{V}_c = [\mathbf{V}_{\text{task}}; \mathbf{V}_{\text{clip}}]$:

$$\text{Attn}(\mathbf{Q}, \mathbf{K}_c, \mathbf{V}_c) = \text{Softmax}\left(\frac{\mathbf{Q}\mathbf{K}_c^\top}{\sqrt{d}}\right)\mathbf{V}_c. \quad (3)$$

The task condition conveys *what*, *where*, and *how* to edit, while the CLIP feature reinforces garment appearance. Their fusion enables semantically precise editing with faithful garment transfer across video frames.

3.5 Training Objective

We optimize UniVVT in latent space using conditional flow matching (Esser et al. 2024). Let $\mathbf{x}_0 \sim p_{\text{data}}$ be a clean target-video latent drawn from the latent data distribution p_{data}, $\boldsymbol{\epsilon} \sim \mathcal{N}(\mathbf{0}, \mathbf{I})$ be standard Gaussian noise with identity covariance $\mathbf{I}$, and $t \sim \mathcal{U}(0, 1)$ be a uniformly sampled time step. The linear probability path and its target velocity are

$$\mathbf{x}_t = (1-t)\mathbf{x}_0 + t\boldsymbol{\epsilon}, \qquad \mathbf{v}_t = \boldsymbol{\epsilon} - \mathbf{x}_0. \quad (4)$$

Let $\mathbf{c} = (\mathbf{z}_{\text{video}}, \mathbf{z}_{\text{gar}}, \mathbf{c}_{\text{proj}}, \mathbf{f}_{\text{clip}})$ denote the complete conditioning set, comprising source-video structure, target-garment appearance, and task-aware semantics. We optimize the conditional velocity predictor $\mathcal{G}_\phi$ using

$$\mathcal{L} = \mathbb{E}_{\mathbf{x}_0, \boldsymbol{\epsilon}, t}\left[\|\mathcal{G}_\phi(\mathbf{x}_t, \mathbf{c}, t) - \mathbf{v}_t\|_2^2\right]. \quad (5)$$

This objective fits the conditional vector field along the data–noise path. At inference, integrating the learned field in reverse transports noise toward a target-video latent while preserving the source motion and scene and faithfully transferring the target garment.

3.6 Progressive Training Strategy

Training UniVVT end to end is challenging because the perceiver and generator originate from distinct pretrained models, while the semantic bridge is initialized from scratch. Their disparate representation spaces and optimization dynamics make naive joint training unstable and yield weak cross-module alignment. We therefore progressively adapt the framework in three stages.

Stage 1: Semantic alignment. We first freeze the video generator $\mathcal{G}_\phi$, optimize the semantic bridge $\mathcal{P}_\theta$, and adapt the MLLM π_{mllm} using Low-Rank Adaptation (LoRA) (Hu et al. 2022). With the generator serving as a fixed target interface, the perceiver and bridge learn to produce task-aware conditions compatible with its conditioning space. This stage establishes a reliable semantic interface for stable and effective subsequent joint training.

Stage 2: Joint end-to-end adaptation. We then jointly optimize the VVT objective by applying LoRA to both π_{mllm} and $\mathcal{G}_\phi$ while fully training $\mathcal{P}_\theta$. Training at a base resolution of 512×384 controls memory cost and improves optimization efficiency. This joint adaptation co-adapts perception, alignment, and generation, enabling faithful garment transfer and temporally coherent synthesis.

Stage 3: Flexible-resolution refinement. Finally, we freeze π_{mllm} and $\mathcal{P}_\theta$ and continue fine-tuning the LoRA parameters of $\mathcal{G}_\phi$ from the Stage 2 checkpoint, using randomly sampled resolutions from 256p to 1024p. This stage improves fidelity and scale robustness without disrupting the semantic alignment learned in earlier stages.

Together, this curriculum decomposes the difficult coupling of heterogeneous pretrained models into semantic alignment, end-to-end co-adaptation, and resolution refinement. It progressively turns MLLM semantics into effective generative control, yielding stable optimization, faithful garment transfer, and flexible-resolution synthesis.

4 Experiments

4.1 Datasets

We train UniVVT on a mixed image–video corpus consisting of VITON-HD (11,647 pairs at 768×1024) (Choi et al. 2021), DressCode (48,392 pairs at 768×1024) (Morelli et al. 2022), and ViViD (7,759 pairs at 624×832) (Fang et al. 2024b). Our training formulation requires source–target pairs of the same subject with consistent pose or motion but different garments, which are hard to collect. We thus train separate DensePose-conditioned inpainters for images and videos to synthesize only source inputs and construct $\langle$*source*, *garment*, *target*$\rangle$ triplets. All garment references and ground-truth targets come from original datasets, meaning UniVVT is supervised purely by real images and videos. DensePose is limited to offline data construction and unused during inference. Adopting official train-test splits, we evaluate DressCode and VITON-HD with standard image-level protocols and ViViD-S (Chong et al. 2025) with the video-level protocol under both paired and unpaired settings.

4.2 Evaluation Metrics

For image try-on, we use FID (2020) and KID (2018) to measure distribution-level realism. Under paired settings, we additionally report SSIM (2004) and LPIPS (2018) for structural and perceptual similarity, respectively. For video try-on, we report VFID computed with I3D (2017) and ResNeXt (2017) backbones, denoted as VFID_{I} and VFID_{R}. Paired video evaluation further includes frame-level SSIM and LPIPS.

4.3 Implementation Details

We conduct all experiments on eight NVIDIA A100 GPUs. The scene-task perceiver and video generator are initialized from Qwen3-VL-2B-Instruct (2025) and Wan2.1-Fun-Control (2025), respectively, with $N = 512$ task queries. We optimize the model using AdamW (2017) with a constant learning rate of 1×10^{-4}, weight decay of 0.01, LoRA rank of 32, and a per-GPU batch size of 1. Each training stage runs for 30k steps. Stages 1 and 2 use a resolution of 512×384, whereas Stage 3 performs multi-resolution training. At inference, we adopt the Euler scheduler (2022) with 28 sampling steps and a fixed random seed of 42. For fair comparison, all quantitative results are reported at 512×384, although UniVVT supports higher-resolution synthesis.

Method	Paradigm	Paired				Unpaired	
		$VFID_I \downarrow$	$VFID_R \downarrow$	SSIM ↑	LPIPS ↓	$VFID_I \downarrow$	$VFID_R \downarrow$
StableVITON + AM (2024)	Pre+Inp+AM	34.2446	0.7735	0.8019	0.1338	36.8985	0.9064
OOTDiffusion + AM (2025)	Pre+Inp+AM	29.5253	3.9372	0.8087	0.1232	35.3170	5.7078
IDM-VTON + AM (2024)	Pre+Inp+AM	20.0812	0.3674	0.8227	0.1163	25.4972	0.7167
ViViD (2024b)	Pre+Inp	17.2924	0.6209	0.8029	0.1221	21.8032	0.8212
CatV^{2}TON (2025)	Pre+Inp	13.5962	0.2963	0.8727	0.0639	19.5131	0.5283
OIE (2025)	Pre+Inp	9.3983	–	0.8466	0.0774	17.0831	–
DreamVVT (2025)	Pre+Inp	11.0180	0.2549	0.8737	0.0619	16.9468	0.4285
MagicTryOn (2025)	Pre+Inp	<u>8.4030</u>	<u>0.2346</u>	**0.9011**	<u>0.0602</u>	<u>14.7174</u>	<u>0.3200</u>
Ours	**End2End**	**8.3623**	**0.1934**	<u>0.8922</u>	**0.0456**	**12.3640**	**0.1876**

Table 1: Quantitative results on ViViD-S under paired and unpaired settings. Arrows indicate the preferred direction. Best and second-best results are bold and underlined, respectively. Pre, Inp, and AM denote preprocessing, inpainting, and animation.

Method	Paired				Unpaired	
	FID ↓	KID ↓	SSIM ↑	LPIPS ↓	FID ↓	KID ↓
GP-VTON	9.927	4.610	0.7711	0.1801	12.792	6.627
LaDI-VTON	9.555	4.683	0.7656	0.2366	10.676	5.787
IDM-VTON	6.821	2.924	0.8797	0.0563	9.546	4.320
OOTDiffusion	4.610	0.955	0.8854	0.0533	12.567	6.627
CatVTON	3.992	0.818	0.8922	0.0455	6.137	1.549
CatV^{2}TON	5.722	2.338	**0.9222**	<u>0.0367</u>	8.627	3.838
MagicTryOn	<u>3.356</u>	<u>0.6851</u>	0.9032	0.04215	<u>5.314</u>	<u>1.339</u>
Ours	**2.734**	**0.4154**	<u>0.9130</u>	**0.0349**	**4.900**	**0.960**

Table 2: Quantitative results on DressCode under paired and unpaired settings. Arrows indicate the preferred direction; best and second-best results are bold and underlined.

Method	Paired				Unpaired	
	FID ↓	KID ↓	SSIM ↑	LPIPS ↓	FID ↓	KID ↓
GP-VTON	8.726	3.944	0.8701	0.0585	11.844	4.310
LaDI-VTON	11.386	7.248	0.8603	0.0733	14.648	8.754
IDM-VTON	6.338	1.322	0.8806	0.0789	9.611	1.639
OOTDiffusion	9.305	4.086	0.8187	0.0876	12.408	4.689
CatVTON	6.139	0.964	0.8691	0.0973	<u>9.143</u>	1.267
CatV^{2}TON	8.095	2.245	**0.8902**	0.0572	11.222	2.986
MagicTryOn	<u>5.689</u>	<u>0.710</u>	0.8804	<u>0.0526</u>	9.203	<u>1.217</u>
Ours	**5.348**	**0.3667**	<u>0.8821</u>	**0.0512**	**9.014**	**1.130**

Table 3: Quantitative results on VITON-HD under paired and unpaired settings. Arrows indicate the preferred direction; best and second-best results are bold and underlined.

4.4 Quantitative Experiments

Performance. Table 1 reports quantitative results on the ViViD-S video try-on benchmark. UniVVT delivers the best overall performance on most metrics: it achieves the lowest $VFID_I$ and $VFID_R$ under both paired and unpaired settings, indicating improved video realism and closer alignment with the real-data distribution. Under paired evaluation, UniVVT obtains the best LPIPS and a competitive SSIM, demonstrating strong perceptual quality and structural consistency. Tables 2 and 3 present results on the DressCode and VITON-HD image try-on benchmarks. UniVVT consistently achieves the best or second-best performance across FID, KID, SSIM, and LPIPS, demonstrating consistent effectiveness across video and image try-on. Notably, the competing methods rely on explicit preprocessing and inpainting-based generation, whereas UniVVT performs end-to-end conditional synthesis without such modules at inference. These results validate the effectiveness of unifying task understanding and generation while eliminating fragile upstream dependencies.

Latency analysis. Figure 3 compares the conditioning overhead of frame-wise geometric preprocessing, including mask and DensePose extraction, with UniVVT's implicit task encoding. As the video length increases from 30 to 90 frames, explicit preprocessing grows nearly linearly from 36.36 s to 111.39 s, whereas UniVVT increases only from 2.06 s to 2.92 s. UniVVT therefore delivers a **17.7–38.1**× speedup, with the advantage widening as videos become longer; for

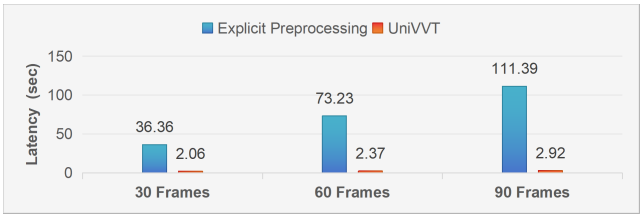


Figure 3: Conditioning latency versus video length. Explicit geometric preprocessing scales nearly linearly, while UniVVT's implicit task encoding grows only marginally.

90 frames, it removes 108.47 s of preprocessing overhead. This gain is architectural rather than merely implementational: replacing dense frame-wise geometry extraction with a compact semantic representation fundamentally improves scalability while preserving end-to-end task awareness.

4.5 Qualitative Experiments

Visual comparision. Figure 4 provides visual comparisons between UniVVT and recent video virtual try-on methods under the unpaired setting on ViViD-S. UniVVT generates outputs with sharper garment textures and stronger temporal consistency. By contrast, ViViD and CatV^{2}TON frequently suffer from blurred textures, missing details, and boundary artifacts. Although MagicTryOn alleviates some defects via fine-grained feature modeling, incomplete garment replacement still occurs when mask estimation is inaccurate. Figure 7 further evaluates image try-on performance

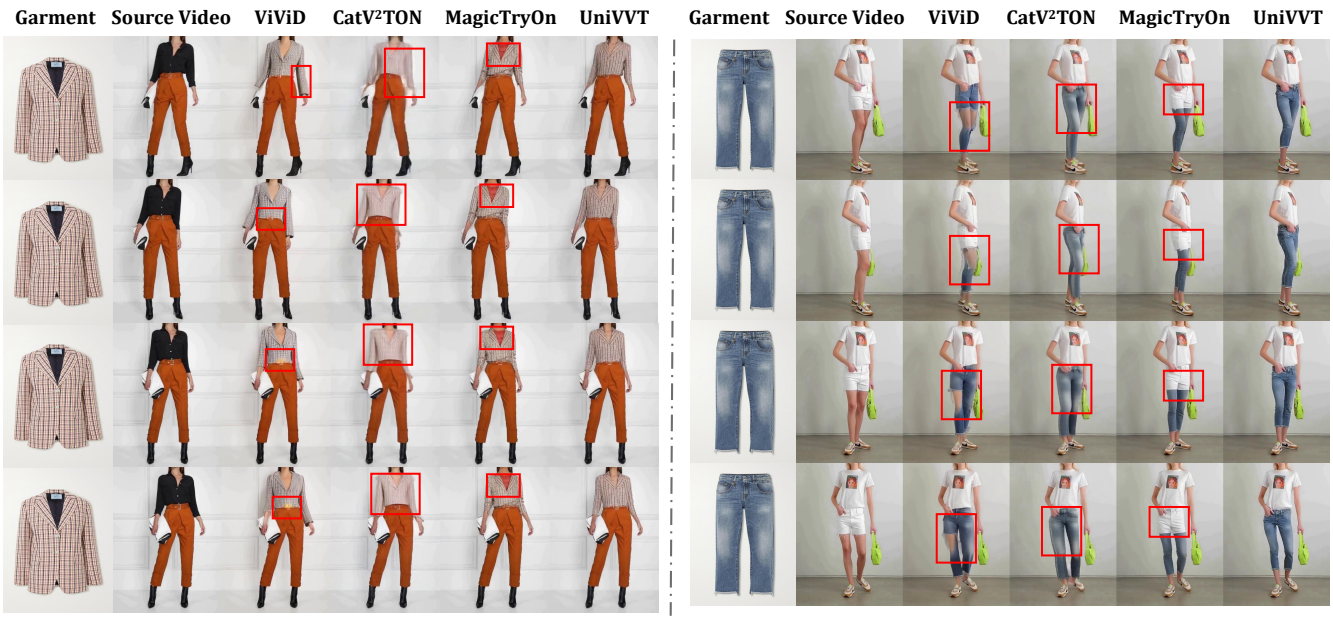


Figure 4: Qualitative comparison on the ViViD-S benchmark under unpaired settings. Compared with baseline methods, UniVVT produces videos with higher visual fidelity and better garment consistency. Please zoom in for better visualization.

for diverse garment categories on DressCode and VITON-HD. UniVVT accurately locates editing regions, preserves human poses and background content, and faithfully transfers the color, texture, and style of reference garments. In comparison, IDM-VTON and CatVTON struggle to retain garment styles, while OOTDiffusion tends to introduce structural artifacts. These observations demonstrate that UniVVT avoids reliance on fragile preprocessing at inference and mitigates try-on failures caused by upstream error propagation, highlighting the benefit of end-to-end optimization.

In-the-wild video try-on. Figure 5 presents UniVVT try-on results on in-the-wild TikTok dance videos. These complex dynamic scenes are out-of-distribution (OOD) relative to our training data, with no corresponding samples used during optimization. UniVVT nevertheless adapts well to such unseen real-world settings, demonstrating strong generalization and robustness.

Interpretation via attention visualization. Why can UniVVT localize the spatio-temporal edit region without an explicit mask prior? Unlike conventional pipelines that hard-constrain synthesis with garment masks, UniVVT conditions the generator with a compact task representation. We visualize the cross-attention of $\mathbf{z}_{\text{task}}$ over the denoised latents during generation (Figure 6). For a long-sleeved target, attention concentrates on the upper body and remains high along the arms across frames, while responses on the face and background stay comparatively weak. This indicates that $\mathbf{z}_{\text{task}}$ jointly encodes *what* to transfer, *where* to edit, and *how* to maintain appearance over time, acting as an implicit semantic guide that enables precise try-on without mask supervision.



Figure 5: In-the-wild try-on results of UniVVT on dance videos with complex motion.

Method	Paired				Unpaired	
	$\text{VFID}_\text{I}\downarrow$	$\text{VFID}_\text{R}\downarrow$	SSIM↑	LPIPS↓	$\text{VFID}_\text{I}\downarrow$	$\text{VFID}_\text{R}\downarrow$
UniVVT	**8.3623**	**0.1934**	**0.8922**	**0.0456**	**12.3640**	**0.1876**
w/o STP	11.7308	0.2282	0.8509	0.0752	14.2424	0.4424

Table 4: Ablation study of the STP module on ViViD-S. Arrows indicate the preferred direction; best results are bold.

4.6 Ablation Studies

Necessity of the scene-task perceiver. The scene-task perceiver (STP) maps multimodal inputs into a compact task latent $\mathbf{z}_{\text{task}}$ that captures overall try-on intent. To assess its necessity, we replace STP with a text-only encoder, yielding the variant **w/o STP**. As shown in Table 4, this change degrades all metrics under both paired and unpaired settings. Figure 8 further shows that, without STP, the model loses holistic task understanding and fails to localize valid edit regions. For example, a short skirt is incorrectly placed on the

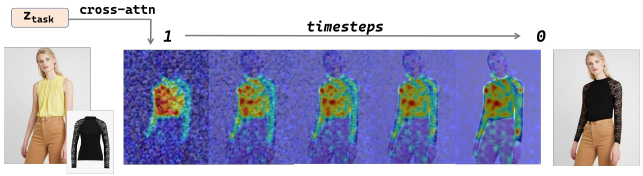


Figure 6: Cross-attention of $\mathbf{z}_{\text{task}}$ over denoised latents. Attention focuses on the editable garment region while remaining weak on identity and background.



Figure 7: Qualitative comparison on VITON-HD (top two rows) and DressCode (bottom three rows). UniVVT better preserves garment appearance, pose, and background.

upper body (row 1), and only the upper half of a target dress is transferred while the lower body remains unchanged (row 3). These results confirm that STP is critical for macroscopic task understanding and intent control in virtual try-on.

Effect of progressive training. Table 5 reports quantitative scores under the paired setting after each training stage. Stage 1 aligns the MLLM and generator conditioning spaces with a frozen DiT backbone; the large residual gap to real data shows that semantic alignment alone is insufficient. Stage 2 jointly adapts all components at 512×384 and yields the main gains in distributional realism and garment fidelity. Stage 3 then refines the generator under multi-resolution sampling, further improving SSIM and LPIPS at 256×192 and 832×624 while preserving competitive quality at the base resolution. Overall, the curriculum progressively converts cross-module alignment into stable VVT performance and resolution flexibility.

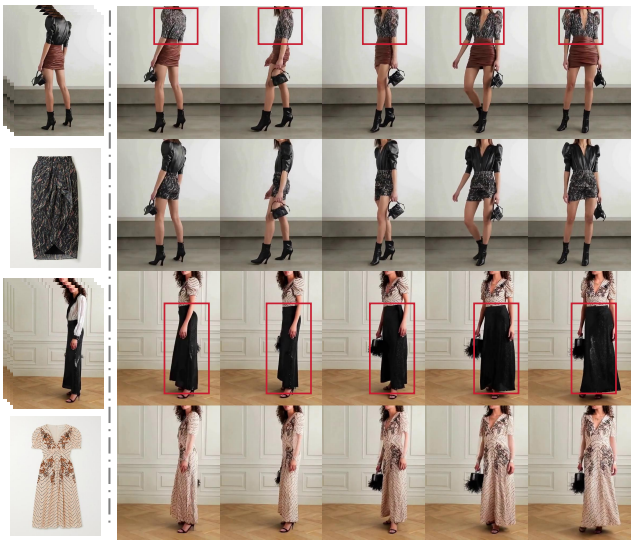


Figure 8: Qualitative ablation of the scene-task perceiver. Left: source video and reference garment; right: w/o STP (rows 1 and 3) vs. UniVVT (rows 2 and 4).

Phase	Resolution	Paired			
		$\text{VFID}_{\text{I}} \downarrow$	$\text{VFID}_{\text{R}} \downarrow$	SSIM $\uparrow$	LPIPS $\downarrow$
Stage 1	512×384	21.5989	1.9006	0.6723	0.1873
Stage 2	256×192	8.7705	0.1804	0.8668	0.0476
	512×384	8.3050	0.1981	0.8923	0.0454
	832×624	8.5018	0.1702	0.8760	0.0597
Stage 3	256×192	8.8597	**0.1778**	**0.8896**	**0.0382**
	512×384	8.3623	0.1934	0.8922	0.0456
	832×624	**8.2969**	0.1774	**0.9062**	**0.0586**

Table 5: Stage-wise progressive training results on ViViD-S (paired). Arrows indicate the preferred direction; bold marks Stage 3 gains at non-default resolutions.

5 Conclusion

We present UniVVT, a unified end-to-end framework that reformulates video virtual try-on as semantically conditioned video generation rather than mask-conditioned inpainting. An MLLM-based scene-task perceiver and a lightweight semantic bridge convert the source video, target garment, and instruction into compact implicit guidance of *what*, *where*, and *how* to edit, removing fragile mask, pose, and warping modules at inference, while a three-stage progressive training strategy stably couples these heterogeneous pretrained components for reliable try-on synthesis. Extensive experiments on video and image benchmarks show that UniVVT delivers strong garment fidelity and temporal consistency across diverse garments and motion without sacrificing identity or scene context, establishing end-to-end joint optimization with implicit semantic guidance as a practical alternative to multi-stage pipelines limited by disjoint component-wise training and brittle geometric preprocessing.

References

Bai, S.; Cai, Y.; Chen, R.; et al. 2025. Qwen3-VL Technical Report. *arXiv preprint arXiv:2511.21631*.

Bińkowski, M.; Sutherland, D. J.; Arbel, M.; and Gretton, A. 2018. Demystifying MMD GANs. *International Conference on Learning Representations (ICLR)*.

Blattmann, A.; Rombach, R.; Ling, H.; Dockhorn, T.; Kim, S. W.; Fidler, S.; et al. 2023. Align your latents: High-resolution video synthesis with latent diffusion models. In *Proceedings of the IEEE/CVF Conference on Computer Vision and Pattern Recognition (CVPR)*, 22563–22575.

Bookstein, F. L. 2002. Principal warps: Thin-plate splines and the decomposition of deformations. *IEEE Transactions on Pattern Analysis and Machine Intelligence*, 11(6): 567–585.

Brooks, T.; Holynski, A.; and Efros, A. A. 2023. Instructpix2pix: Learning to follow image editing instructions. In *Proceedings of the IEEE/CVF Conference on Computer Vision and Pattern Recognition (CVPR)*, 18392–18402.

Carreira, J.; and Zisserman, A. 2017. Quo Vadis, Action Recognition? A New Model and the Kinetics Dataset. In *Proceedings of the IEEE/CVF Conference on Computer Vision and Pattern Recognition (CVPR)*, 6299–6308.

Cheng, X.; Zeng, W.; Dai, D.; Chen, Q.; Wang, B.; Xie, Z.; et al. 2026. Conditional memory via scalable lookup: A new axis of sparsity for large language models. *arXiv preprint arXiv:2601.07372*.

Cherti, M.; Beaumont, R.; Wightman, R.; Wortsman, M.; Ilharco, G.; Gordon, C.; et al. 2023. Reproducible scaling laws for contrastive language-image learning. In *Proceedings of the IEEE/CVF Conference on Computer Vision and Pattern Recognition (CVPR)*, 2818–2829.

Choi, S.; Park, S.; Lee, M.; and Choo, J. 2021. VITON-HD: High-Resolution Virtual Try-On via Misalignment-Aware Normalization. In *Proceedings of the IEEE/CVF Conference on Computer Vision and Pattern Recognition (CVPR)*, 14131–14140.

Choi, Y.; Kwak, S.; Lee, K.; Choi, H.; and Shin, J. 2024. Improving diffusion models for authentic virtual try-on in the wild. In *Proceedings of the European Conference on Computer Vision (ECCV)*, 206–235.

Chong, Z.; Dong, X.; Li, H.; Zhang, S.; Zhang, W.; Zhang, X.; et al. 2024. Catvton: Concatenation is all you need for virtual try-on with diffusion models. *arXiv preprint arXiv:2407.15886*.

Chong, Z.; Zhang, W.; Zhang, S.; Zheng, J.; Dong, X.; Li, H.; et al. 2025. Catv2ton: Taming diffusion transformers for vision-based virtual try-on with temporal concatenation. *arXiv preprint arXiv:2501.11325*.

Comanici, G.; Bieber, E.; Schaekermann, M.; Pasupat, I.; Sachdeva, N.; Dhillon, I.; et al. 2025. Gemini 2.5: Pushing the frontier with advanced reasoning, multimodality, long context, and next generation agentic capabilities. *arXiv preprint arXiv:2507.06261*.

Deng, Z.; Ma, W.; Han, Q.-L.; Zhou, W.; Zhu, X.; Wen, S.; et al. 2025. Exploring DeepSeek: A survey on advances, applications, challenges and future directions. *IEEE/CAA Journal of Automatica Sinica*, 12(5): 872–893.

Dong, H.; Liang, X.; Shen, X.; Wu, B.; Chen, B.-C.; and Yin, J. 2019. Fw-gan: Flow-navigated warping gan for video virtual try-on. In *Proceedings of the IEEE/CVF International Conference on Computer Vision (ICCV)*, 1161–1170.

Esser, P.; Kulal, S.; Blattmann, A.; Entezari, R.; Müller, J.; Saini, H.; et al. 2024. Scaling rectified flow transformers for high-resolution image synthesis. In *Proceedings of the International Conference on Machine Learning (ICML)*.

Fang, N.; Qiu, L.; Zhang, S.; Wang, Z.; and Hu, K. 2024a. PG-VTON: A novel image-based virtual try-on method via progressive inference paradigm. *IEEE Transactions on Multimedia*, 26: 6595–6608.

Fang, Z.; Zhai, W.; Su, A.; Song, H.; Zhu, K.; Wang, M.; et al. 2024b. Vivid: Video virtual try-on using diffusion models. *arXiv preprint arXiv:2405.11794*.

Ge, Y.; Song, Y.; Zhang, R.; Ge, C.; Liu, W.; and Luo, P. 2021. Parser-free virtual try-on via distilling appearance flows. In *Proceedings of the IEEE/CVF Conference on Computer Vision and Pattern Recognition (CVPR)*, 8485–8493.

Han, X.; Hu, X.; Huang, W.; and Scott, M. R. 2019. Clothflow: A flow-based model for clothed person generation. In *Proceedings of the IEEE/CVF International Conference on Computer Vision (ICCV)*, 10471–10480.

Hu, E. J.; Shen, Y.; Wallis, P.; Allen-Zhu, Z.; Li, Y.; Wang, S.; et al. 2022. Lora: Low-rank adaptation of large language models. *International Conference on Learning Representations (ICLR)*, 1(2): 3.

Jiang, B.; Hu, X.; Luo, D.; He, Q.; Xu, C.; Peng, J.; et al. 2024. Fitdit: Advancing the authentic garment details for high-fidelity virtual try-on. *arXiv preprint arXiv:2411.10499*.

Jiang, J.; Wang, T.; Yan, H.; and Liu, J. 2022. Clothformer: Taming video virtual try-on in all module. In *Proceedings of the IEEE/CVF Conference on Computer Vision and Pattern Recognition (CVPR)*, 10799–10808.

Karras, J.; Li, Y.; Liu, N.; Zhu, L.; Yoo, I.; Lugmayr, A.; et al. 2024. Fashion-vdm: Video diffusion model for virtual try-on. In *SIGGRAPH Asia 2024 Conference Papers*, 1–11.

Karras, T.; Aittala, M.; Aila, T.; and Laine, S. 2022. Elucidating the design space of diffusion-based generative models. *Advances in Neural Information Processing Systems (NeurIPS)*, 35: 26565–26577.

Kim, J.; Gu, G.; Park, M.; Park, S.; and Choo, J. 2024. Stableviton: Learning semantic correspondence with latent diffusion model for virtual try-on. In *Proceedings of the IEEE/CVF Conference on Computer Vision and Pattern Recognition (CVPR)*, 8176–8185.

Labs, B. F. 2025. FLUX. 2: Frontier Visual Intelligence. *https://bfl. ai/blog/flux-2*.

Li, G.; Zheng, S.; Zhang, H.; Chen, J.; Luan, J.; Ou, B.; et al. 2025. MagicTryOn: Harnessing Diffusion Transformer for Garment-Preserving Video Virtual Try-on. *arXiv preprint arXiv:2505.21325*.

Loshchilov, I.; and Hutter, F. 2017. Decoupled weight decay regularization. *arXiv preprint arXiv:1711.05101*.

Minar, M. R.; Tuan, T. T.; Ahn, H.; Rosin, P.; and Lai, Y.-K. 2020. Cp-vton+: Clothing shape and texture preserving image-based virtual try-on. In *CVPR Workshops*, volume 3, 10–14.

Morelli, D.; Baldrati, A.; Cartella, G.; Cornia, M.; Bertini, M.; and Cucchiara, R. 2023. Ladi-vton: Latent diffusion textual-inversion enhanced virtual try-on. In *Proceedings of the ACM International Conference on Multimedia (ACM MM)*, 8580–8589.

Morelli, D.; Fincato, M.; Cornia, M.; Landi, F.; Cesari, F.; and Cucchiara, R. 2022. Dress Code: High-Resolution Multi-Category Virtual Try-On. In *Proceedings of the European Conference on Computer Vision (ECCV)*, 345–362.

Mou, C.; Sun, Q.; Wu, Y.; Zhang, P.; Li, X.; Ye, F.; et al. 2025. Instructx: Towards unified visual editing with mllm guidance. *arXiv preprint arXiv:2510.08485*.

Pan, Y.; He, Q.; Wang, L.; Peng, B.; and Chi, M. 2025. Once Is Enough: Lightweight DiT-Based Video Virtual Try-On via One-Time Garment Appearance Injection. *arXiv preprint arXiv:2510.07654*.

Qwen Team. 2026. Qwen3.5: Towards Native Multimodal Agents.

Seitzer, M. 2020. pytorch-fid: FID Score for PyTorch. *GitHub repository*.

Singh, A.; Fry, A.; Perelman, A.; Tart, A.; Ganesh, A.; El-Kishky, A.; et al. 2025. Openai gpt-5 system card. *arXiv preprint arXiv:2601.03267*.

Song, D.; Zhang, X.; Zhou, J.; Nie, W.; Tong, R.; Kankanhalli, M.; et al. 2025. Image-based virtual try-on: A survey. *International Journal of Computer Vision*, 133(5): 2692–2720.

Taseer, M. A. 2024. xMGIE: Advanced MLLM-Guided Image Editing with Progressive Feature Blending, Cross-Attention Masking, Identity Embeddings, and Gaussian Blurring. *arXiv preprint*.

Velioglu, R.; Bevandic, P.; Chan, R.; and Hammer, B. 2024. Tryoffdiff: Virtual-try-off via high-fidelity garment reconstruction using diffusion models. *arXiv preprint arXiv:2411.18350*.

Wang, A.; Ai, B.; et al. 2025. Wan: Open and Advanced Large-Scale Video Generative Models. *arXiv preprint arXiv:2503.20314*.

Wang, S.; Zhao, J.; Cui, Y.; Zhang, C.; and Li, X. 2024. MAGiC: An LLM-Powered Multi-Agent Framework for Unleashing Visual Creativity. *arXiv preprint*.

Wang, Z.; Bovik, A. C.; Sheikh, H. R.; and Simoncelli, E. P. 2004. Image Quality Assessment: From Error Visibility to Structural Similarity. *IEEE Transactions on Image Processing*, 13(4): 600–612.

Wang, Z.; Sun, X.; Wu, S.; Zhan, J.; Si, J.; Zhang, C.; et al. 2025. FW-VTON: Flattening-and-Warping for Person-to-Person Virtual Try-on. *arXiv preprint arXiv:2507.16010*.

Xie, S.; Girshick, R.; Dollár, P.; Tu, Z.; and He, K. 2017. Aggregated Residual Transformations for Deep Neural Networks. In *Proceedings of the IEEE/CVF Conference on Computer Vision and Pattern Recognition (CVPR)*, 1492–1500.

Xing, J.; Xu, C.; Qian, Y.; Liu, Y.; Dai, G.; Sun, B.; et al. 2025. Tryon-adapter: Efficient fine-grained clothing identity adaptation for high-fidelity virtual try-on. *International Journal of Computer Vision*, 133(6): 3781–3802.

Xu, Y.; Gu, T.; Chen, W.; and Chen, A. 2025. Ootdiffusion: Outfitting fusion based latent diffusion for controllable virtual try-on. In *Proceedings of the AAAI Conference on Artificial Intelligence (AAAI)*, volume 39, 8996–9004.

Yang, H.; Zhang, R.; Guo, X.; Liu, W.; Zuo, W.; and Luo, P. 2020. Towards photo-realistic virtual try-on by adaptively generating-preserving image content. In *Proceedings of the IEEE/CVF Conference on Computer Vision and Pattern Recognition (CVPR)*, 7850–7859.

Yang, Z.; Jiang, Z.; Li, X.; Zhou, H.; Dong, J.; Zhang, H.; et al. 2024. D4-VTON: Dynamic Semantics Disentangling for Differential Diffusion Based Virtual Try-On. In *Proceedings of the European Conference on Computer Vision (ECCV)*, 36–52.

Yuan, Y.; Chen, H.; and Ng, C. 2025. Instruction tuning for story understanding and generation with weak supervision. *arXiv preprint arXiv:2501.15574*.

Zhang, R.; Isola, P.; Efros, A. A.; Shechtman, E.; and Wang, O. 2018. The Unreasonable Effectiveness of Deep Features as a Perceptual Metric. In *Proceedings of the IEEE/CVF Conference on Computer Vision and Pattern Recognition (CVPR)*, 586–595.

Zhang, W.; Jin, Y.; Li, X.; Zhang, Y.; Cong, X.; Wang, C.; et al. 2026. UniFit: Towards Universal Virtual Try-on with MLLM-Guided Semantic Alignment. In *Proceedings of the AAAI Conference on Artificial Intelligence (AAAI)*, volume 40, 12816–12824.

Zhao, B.; Wu, C.; Li, D.; Meng, H.; Li, J.; Zhang, J.; Zhou, J.; Lin, J.; Gao, K.; Cao, K.; et al. 2026. Qwen-image-2.0 technical report. *arXiv preprint arXiv:2605.10730*.

Zhao, X.; Ding, S.; Zhang, Z.; Huang, H.; Maosongcao, M.; Wang, J.; et al. 2025. Omnialign-v: Towards enhanced alignment of mllms with human preference. In *Proceedings of the Annual Meeting of the Association for Computational Linguistics (ACL)*, 18490–18515.

Zheng, J.; Wang, J.; Zhao, F.; Zhang, X.; and Liang, X. 2024. Dynamic try-on: Taming video virtual try-on with dynamic attention mechanism. *arXiv preprint arXiv:2412.09822*.

Zhong, X.; Wu, Z.; Tan, T.; Lin, G.; and Wu, Q. 2021. Mv-ton: Memory-based video virtual try-on network. In *Proceedings of the ACM International Conference on Multimedia (ACM MM)*, 908–916.

Zhu, L.; Yang, D.; Zhu, T.; Reda, F.; Chan, W.; Saharia, C.; et al. 2023. Tryondiffusion: A tale of two unets. In *Proceedings of the IEEE/CVF Conference on Computer Vision and Pattern Recognition (CVPR)*, 4606–4615.

Zou, C.; Cheng, S.; Xu, B.; Zheng, D.; Li, X.; Chen, J.; et al. 2025. Video Virtual Try-on with Conditional Diffusion Transformer Inpainter. *arXiv preprint arXiv:2506.21270*.

Zuo, T.; Huang, Z.; Ning, S.; Lin, E.; Liang, C.; Zheng, Z.; et al. 2025. Dreamvvt: Mastering realistic video virtual try-on in the wild via a stage-wise diffusion transformer framework. *arXiv preprint arXiv:2508.02807*.

This appendix complements the main paper with further analyses and implementation details. We first describe the construction of training triplets, and then provide additional ablation studies and additional quantitative and qualitative evaluations, followed by a discussion of the current limitations of UniVVT.

A Training-Triplet Construction

Motivation. Public virtual try-on datasets provide real garment–target pairs $(\mathbf{I}_{\text{gar}}, \mathbf{V}_{\text{out}})$, but UniVVT requires aligned triplets $\langle \mathbf{V}_{\text{in}}, \mathbf{I}_{\text{gar}}, \mathbf{V}_{\text{out}} \rangle$. Ideally, $\mathbf{V}_{\text{in}}$ and $\mathbf{V}_{\text{out}}$ should depict the same person under identical pose, motion, viewpoint, and scene conditions, differing only in the worn garment. Capturing such pairs would require reproducing an entire image or video sequence after a clothing change, which is impractical at scale. Naively pairing unrelated samples would instead entangle garment transfer with changes in identity, motion, camera, and background, weakening the supervision signal.

Triplet construction. We address this data gap by synthesizing the source input rather than the supervision target. As shown in Figure 9, we begin with a real pair $(\mathbf{I}_{\text{gar}}, \mathbf{V}_{\text{out}})$ and sample an alternative garment description that is distinct from the target garment. An inpainting model then replaces the clothing in $\mathbf{V}_{\text{out}}$ according to this description, producing a synthetic source $\mathbf{V}_{\text{in}}$. During synthesis, garment masks localize the editable region, while DensePose conditioning preserves body configuration and frame-to-frame motion. Because identity, pose, camera, and background are inherited from the same real target, the resulting triplet isolates the garment change while minimizing unrelated variation.

Real-target supervision. Importantly, synthesis is restricted to the conditioning side of the training pair. The generated $\mathbf{V}_{\text{in}}$ serves only as an input, whereas $\mathbf{I}_{\text{gar}}$ and the ground-truth $\mathbf{V}_{\text{out}}$ are retained directly from the original dataset. Consequently, every reconstruction and diffusion target is derived from real imagery: UniVVT is optimized to map a synthetic source back to a real target and is never trained to reproduce an inpainted output. The inpainting models therefore act exclusively as offline data-generation tools, rather than teachers, and no teacher–student distillation is involved. This separation enables synthetic editing to resolve the scarcity of aligned triplets without introducing synthetic targets into the supervision.

Synthesis and quality control. We use FLUX.1-dev (Labs 2025) to construct image triplets and Wan2.1-Fun-1.3B-Control (Wang, Ai et al. 2025) to construct video triplets. DensePose maps and garment masks are used only during this offline synthesis procedure; they are not exposed to UniVVT as inputs during either training or inference. Finally, we manually inspect every generated source and discard samples with identity drift, inconsistent motion, mask leakage, incomplete garment replacement, or conspicuous inpainting artifacts. This filtering step ensures that the retained triplets preserve the intended correspondence between source content and real target supervision.

B Additional Ablation Experiments

Complementarity of task semantics and garment appearance. Each DiT block receives two semantic conditions: the projected task representation $\mathbf{c}_{\text{proj}} = \mathcal{P}_\theta(\mathbf{z}_{\text{task}})$, which is inferred jointly from the source video, target garment, and instruction, and the garment feature $\mathbf{f}_{\text{clip}}$, extracted independently by a frozen CLIP image encoder. Although both conditions are fused within the same cross-attention layer, they are intended to serve distinct roles. We isolate their contributions by retraining two variants, each removing one conditioning branch while preserving the architecture and optimization protocol otherwise. Table 6 shows that removing $\mathbf{z}_{\text{task}}$ degrades all metrics substantially: paired VFID_{I} increases from 8.3623 to 11.7308, LPIPS rises from 0.0456 to 0.0752, and unpaired VFID_{R} more than doubles from 0.1876 to 0.4424. In contrast, removing $\mathbf{f}_{\text{clip}}$ produces consistently smaller, yet non-negligible, drops. These results identify the task-aware pathway as the principal source of semantic control. Unlike the source-independent CLIP descriptor, $\mathbf{z}_{\text{task}}$ integrates the complete try-on context and can therefore coordinate *what* garment to transfer with *where* and *how* to apply the edit throughout motion. The localized responses visualized in Figure 6 of the main paper further support this interpretation. Meanwhile, the consistent gains from $\mathbf{f}_{\text{clip}}$ confirm its complementary role in preserving garment-specific category, style, and appearance cues that may be compressed by the task representation. Their combination consequently achieves the best performance across all paired and unpaired metrics.

Adapting the MLLM to video try-on. The pretrained MLLM supplies strong multimodal priors, but its hidden representation is not explicitly optimized for the body–garment correspondence, edit localization, and temporal transfer required by VVT. We therefore adapt the MLLM with LoRA during Stage 1 semantic alignment and Stage 2 joint optimization. To isolate the contribution of this adaptation, we compare against a variant that freezes the MLLM while retaining the same trainable semantic bridge, generator, and optimization schedule. As shown in Table 7, the frozen variant remains competitive, confirming that generic visual–language pretraining already provides a useful foundation. LoRA adaptation nevertheless improves every paired and unpaired metric: for example, paired VFID_{R} decreases from 0.2353 to 0.1934, while unpaired VFID_{I} decreases from 13.2985 to 12.3640. These consistent gains indicate that VVT requires more than generic garment recognition. Task-specific adaptation reorganizes the MLLM features around the complete editing context, enabling the task queries to jointly capture target appearance, source-person structure, spatial edit intent, and motion-aware correspondence. This produces a more actionable representation for the semantic bridge and reduces the burden on downstream modules to infer task structure from a fixed feature space. The progressive schedule further stabilizes this specialization: Stage 1 aligns the adapted representation to a frozen generator, and Stage 2 co-adapts perception and generation end to end. Thus, LoRA serves not merely as parameter-efficient fine-tuning, but as a mechanism for converting general multimodal knowledge

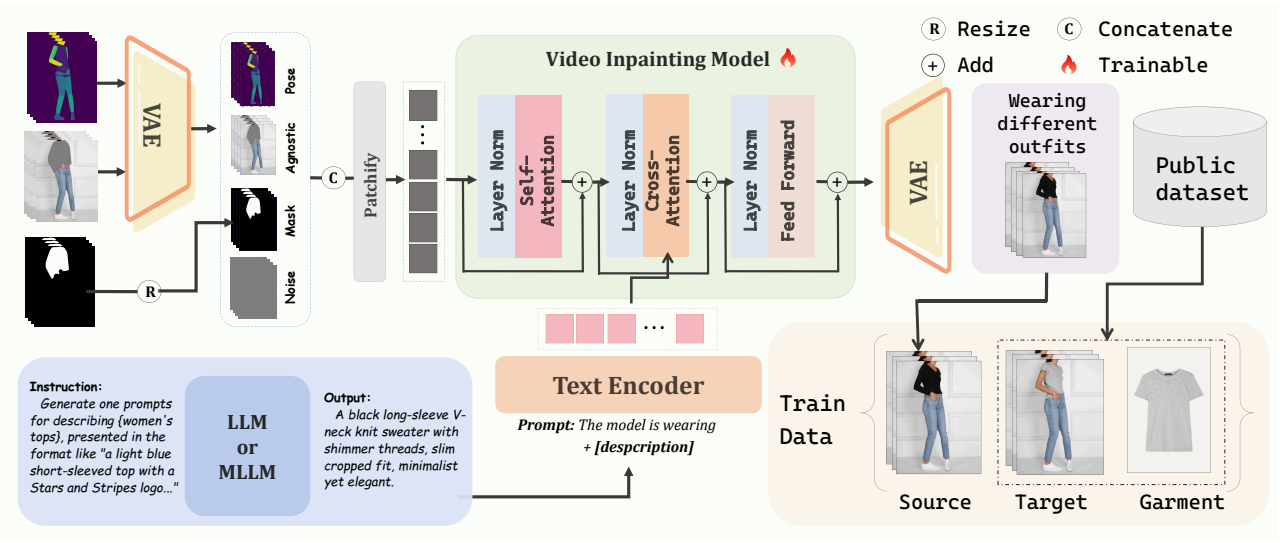


Figure 9: Construction of aligned training triplets using synthetic source inputs and real-target supervision. Starting from a real garment–target pair $(\mathbf{I}_{\text{gar}}, \mathbf{V}_{\text{out}})$, we synthesize $\mathbf{V}_{\text{in}}$ by replacing the clothing in $\mathbf{V}_{\text{out}}$ with an alternative garment specified by an LLM-generated description. Only $\mathbf{V}_{\text{in}}$ is synthesized; $\mathbf{I}_{\text{gar}}$ and $\mathbf{V}_{\text{out}}$ are retained as real samples from the original dataset.

Methods	Paired				Unpaired	
	$\text{VFID}_\text{I}\downarrow$	$\text{VFID}_\text{R}\downarrow$	SSIM↑	LPIPS↓	$\text{VFID}_\text{I}\downarrow$	$\text{VFID}_\text{R}\downarrow$
w/o $\mathbf{z}_{\text{task}}$	11.7308	0.2282	0.8509	0.0752	14.2424	0.4424
w/o $\mathbf{f}_{\text{clip}}$	8.9210	0.1996	0.8843	0.0500	12.5608	0.1985
UniVVT	**8.3623**	**0.1934**	**0.8922**	**0.0456**	**12.3640**	**0.1876**

Table 6: Quantitative ablation of task-aware semantic guidance and CLIP garment conditioning on the ViViD-S video benchmark.

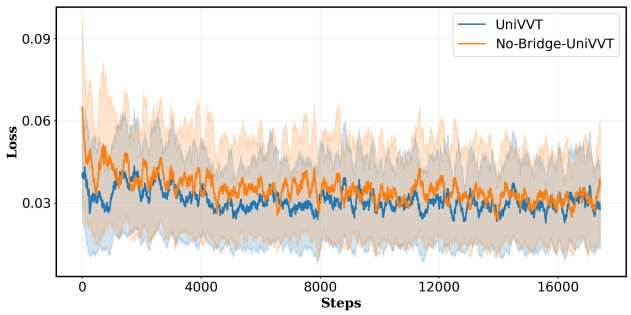


Figure 10: Stage 2 training-loss curves for UniVVT with and without the Semantic Bridge. The learned bridge accelerates convergence and consistently yields a lower optimization loss.

into a task-specific semantic interface for video generation.

Learned alignment between perception and generation. The MLLM and video DiT are pretrained independently and expose incompatible representation spaces. While $\mathbf{z}_{\text{task}}$ encodes multimodal editing intent, the DiT expects conditioning features whose statistics and semantics are compatible with its denoising dynamics. Resolving the dimensional mismatch alone is therefore insufficient. To test whether learned alignment is necessary, we construct *No-Bridge-UniVVT*, which removes $\mathcal{P}_\theta$ and directly injects a zero-padded $\mathbf{z}_{\text{task}}$ while keeping all remaining components and the training schedule unchanged. As reported in Table 8, the Semantic Bridge improves every metric under both evaluation protocols. In particular, unpaired VFID_I decreases from 14.0105 to 12.3640 and VFID_R from 0.2256 to 0.1876, demonstrating stronger generalization beyond matched garment–person pairs. The paired gains in SSIM and LPIPS further show that this improvement is not limited to distribution-level realism, but also extends to structural preservation and perceptual fidelity. Figure 10 provides complementary optimization evidence: the full model converges faster and reaches a consistently lower Stage 2 training loss. Direct injection forces the generator to learn the VVT denoising objective while simultaneously interpreting features from an incompatible MLLM space. The bridge separates these demands by mapping $\mathbf{z}_{\text{task}}$ into generator-compatible tokens $\mathbf{c}_{\text{proj}}$, allowing the DiT to focus on spatially precise and temporally coherent synthesis. This interpretation also motivates the progressive training strategy: Stage 1 learns the cross-model interface against a frozen generator, and Stage 2 subsequently co-adapts perception, alignment, and generation. The Semantic Bridge is thus more than a dimensional projector; it is a lightweight learned interface that converts multimodal task understanding into effective generative control.

LoRA MLLM	Paired				Unpaired	
	$\text{VFID}_\text{I} \downarrow$	$\text{VFID}_\text{R} \downarrow$	SSIM↑	LPIPS↓	$\text{VFID}_\text{I} \downarrow$	$\text{VFID}_\text{R} \downarrow$
✗	8.9187	0.2353	0.8898	0.0488	13.2985	0.2007
✓	**8.3623**	**0.1934**	**0.8922**	**0.0456**	**12.3640**	**0.1876**

Table 7: Ablation of task-specific LoRA adaptation for the MLLM on the ViViD-S video benchmark.

Method	Paired				Unpaired	
	$\text{VFID}_\text{I} \downarrow$	$\text{VFID}_\text{R} \downarrow$	SSIM↑	LPIPS↓	$\text{VFID}_\text{I} \downarrow$	$\text{VFID}_\text{R} \downarrow$
No-Bridge-UniVVT	9.2603	0.1995	0.8807	0.04920	14.0105	0.2256
UniVVT	**8.3623**	**0.1934**	**0.8922**	**0.0456**	**12.3640**	**0.1876**

Table 8: Quantitative ablation results of the semantic bridge module on the ViViD-S video benchmark.

How much capacity does the semantic bridge need? Having established the necessity of a learnable interface, we next investigate whether increasing its capacity further improves semantic alignment. Under the same training protocol and optimization budget, we compare two bridge topologies: a heavy 12-layer Transformer and the lightweight MLP adopted in UniVVT. As shown in Table 9, despite its substantially higher parameter and computational costs, the Transformer surprisingly performs slightly worse than the MLP. This result suggests that the Semantic Bridge need not relearn the complex multimodal reasoning already encoded in the task-aware representation $\mathbf{z}_{\text{task}}$; instead, its primary role is to perform a compact distributional transformation into the generator's conditioning space. Excessive capacity introduces redundant degrees of freedom and lengthens the optimization path across the perceiver–bridge–generator pipeline, potentially making coordinated adaptation more difficult. In contrast, the MLP offers sufficient expressiveness for semantic alignment while retaining a short and stable information pathway. These findings justify our lightweight design as both more effective and substantially more efficient, demonstrating that successful cross-model alignment relies on an appropriately constrained interface rather than maximal bridge capacity.

C Additional Quantitative Experiments

Comparison with recent image-only methods. The main paper has already established the image try-on performance of UniVVT on standard benchmarks. Here, we broaden the comparison to recent image-only systems, including the general-purpose editors Qwen-Image-Edit (Zhao et al. 2026) and FLUX.2-klein (Labs 2025), and the specialized try-on method UniFit (Zhang et al. 2026). UniVVT is designed for video virtual try-on, but its mixed image–video formulation represents an image as a single-frame sequence, allowing the same architecture to operate in the image setting without modality-specific components. In contrast, all compared baselines are restricted to static images and do not support video try-on. Table 10 therefore places a video-oriented unified model against recent methods developed specifically for image editing or image try-on, providing a stricter assessment of its cross-modal compatibility rather than repeating the image capability study from the main paper.

Table 10 shows that the general-purpose editors perform substantially worse on virtual try-on, where the target garment must be reconstructed faithfully while person identity and non-garment content remain unchanged. The specialized UniFit model provides a considerably stronger comparison, yet UniVVT still achieves lower paired FID, KID, and LPIPS, with an essentially identical SSIM of 0.8821 versus 0.883. UniVVT also obtains the best reported FID and KID under the unpaired protocol. Crucially, these image-level results are achieved by a model developed for video try-on and equipped to model temporal dynamics; none of the competing methods supports the video task. UniVVT therefore does not obtain video capability at the expense of static-image quality. Instead, its unified formulation subsumes image try-on as a single-frame case, matching or surpassing dedicated image systems while retaining compatibility with video generation.

D Additional Qualitative Results

Diverse video try-on scenarios. Figure 11 presents additional video results spanning upper-body garments, trousers, and dresses under varied poses, motions, and self-occlusions. UniVVT consistently transfers target color, texture, silhouette, and body coverage while preserving identity, pose, accessories, and background content. In particular, garment appearance remains stable when arms or handbags intermittently occlude the edited region and when the target silhouette differs markedly from the source clothing. These cases require the model to update garment–body correspondence as the person moves rather than applying a fixed spatial edit. Without masks, pose maps, or warped garments at inference, UniVVT infers this correspondence directly from the source video, target garment, and instruction. The resulting spatial precision and cross-frame consistency provide further evidence that task-aware semantic guidance can replace explicit geometric priors across diverse video try-on conditions.

Bidirectional garment-length transfer. Figure 12 examines image try-on under large changes in garment length and spatial coverage, with short-to-long transfers in the top three rows and long-to-short transfers in the bottom three. These cases directly stress the determination of the editing extent: a longer target must synthesize content beyond the

Bridge Design	Params	FLOPs	Paired			
			$\text{VFID}_\text{I}\downarrow$	$\text{VFID}_\text{R}\downarrow$	SSIM↑	LPIPS↓
12-layer Transformer	1260.08M	571.46G	8.8922	0.2026	0.8869	0.0482
MLP	41.96M	21.48G	8.3623	0.1934	0.8922	0.0456

Table 9: Ablation study on the bridge design.

Method	Supports video?	Paired				Unpaired	
		FID↓	KID↓	SSIM↑	LPIPS↓	FID↓	KID↓
Qwen-Image-Edit(Zhao et al. 2026)	✗	14.269	6.1090	0.6976	0.2688	13.5681	5.688
FLUX.2-klein(Labs 2025)	✗	11.503	4.5830	0.8304	0.1189	12.4746	4.1504
UniFit(Zhang et al. 2026)	✗	8.799	0.702	**0.883**	0.065	/	/
UniVVT	✓	**5.348**	**0.3667**	0.8821	**0.0512**	**9.014**	**1.130**

Table 10: Additional comparison with recent image-only editing and try-on methods on VITON-HD. UniVVT is designed for video virtual try-on and is the only model in this comparison that also supports the video setting.

source garment boundary, whereas a shorter target must expose and preserve regions previously covered by the source clothing. Mask-conditioned baselines often inherit their editable support from source-dependent preprocessing. Consequently, they truncate extended sleeves or hems, retain residual long-garment structures, or produce unnatural transitions at the target boundary. UniVVT instead infers the required spatial support jointly from the source person and target garment. It reconstructs long sleeves, trousers, and full-length dresses while also recovering compact tops, skirts, and shorts with cleaner boundaries and more faithful silhouettes. The bidirectional results demonstrate that implicit semantic guidance adapts the editing region to the target garment rather than constraining generation to a predefined source mask.

E Additional Visual Comparisons

Video virtual try-on. Figures 13–15 compare UniVVT with open-source state-of-the-art video try-on methods. Figures 13, 14, and 15 highlight appearance fidelity: UniVVT reconstructs the distinctive paisley print, fine speckled texture, and structured brown patterns with sharper details and more accurate colors, whereas ViViD, CatV2TON, and MagicTryOn often smooth textures, shift colors, or omit characteristic motifs. Figures 16 and 17 expose a complementary weakness of mask-conditioned baselines. Mask errors lead to truncated trousers, blurred leg boundaries, or residual white sleeves and panels from the source garment. By inferring the editing scope directly from the original multimodal inputs, UniVVT produces complete silhouettes, clean garment boundaries, and consistent appearance across frames.

Image virtual try-on. In the image virtual try-on setting, Figures 18, 19, and 20 compare UniVVT on upper-body garments, lower-body garments, and dresses. UniVVT more faithfully preserves neckline and sleeve configurations, garment length and drape, and localized details such as lace, stripes, cargo pockets, and camouflage patterns. Meanwhile, person identity, pose, accessories, and background remain intact. These comparisons demonstrate that UniVVT transfers its unified semantic modeling capability effectively to image virtual try-on, achieving precise garment reconstruction and localized editing across diverse garment categories without an image-specific architecture.

F Limitations and Future Directions

Despite its strong performance, UniVVT retains three limitations that motivate further study.

Temporal stability under extreme motion. Fast body motion, abrupt viewpoint changes, and severe occlusion can induce local texture drift, discontinuous garment patterns, or short-term flicker. The task-aware representation captures global editing intent, but does not explicitly enforce dense correspondence between every pair of adjacent frames. Stronger temporal memory, motion-aware feature propagation, and consistency objectives may therefore improve fine-grained stability in highly dynamic sequences.

Ambiguity in cross-category transfer. Our training data primarily support garment replacement within the same semantic category. Cross-category editing, such as replacing a dress with a top, changes not only garment appearance but also the intended body coverage. As illustrated in Figure 21, the target garment alone does not specify whether regions previously covered by the dress should be preserved, removed, or newly synthesized; none of the evaluated methods resolves this ambiguity reliably. Extending training data to cross-category transformations and introducing finer-grained instructions about the desired outfit composition and editing extent are promising directions.

Inference efficiency. UniVVT eliminates costly frame-wise geometric preprocessing, but iterative diffusion denoising remains the dominant runtime bottleneck. Consequently, the current model is not yet suitable for real-time interactive applications. Few-step distillation, accelerated sampling, and more efficient video-generation backbones could reduce latency while preserving garment fidelity and temporal coherence.



Figure 11: Additional video try-on results across garment categories, motion patterns, and occlusion conditions. The source sequence and target garment are shown on the left, followed by representative generated frames. UniVVT maintains garment appearance and structure over time while preserving the person and scene.



Figure 12: Image try-on under large changes in garment length and spatial coverage (top: short-to-long; bottom: long-to-short). Mask-conditioned baselines frequently inherit an incorrect editing extent from the source garment, whereas UniVVT adapts the edited region to the target and recovers more faithful silhouettes.



Figure 13: Fine-grained pattern preservation in video try-on.

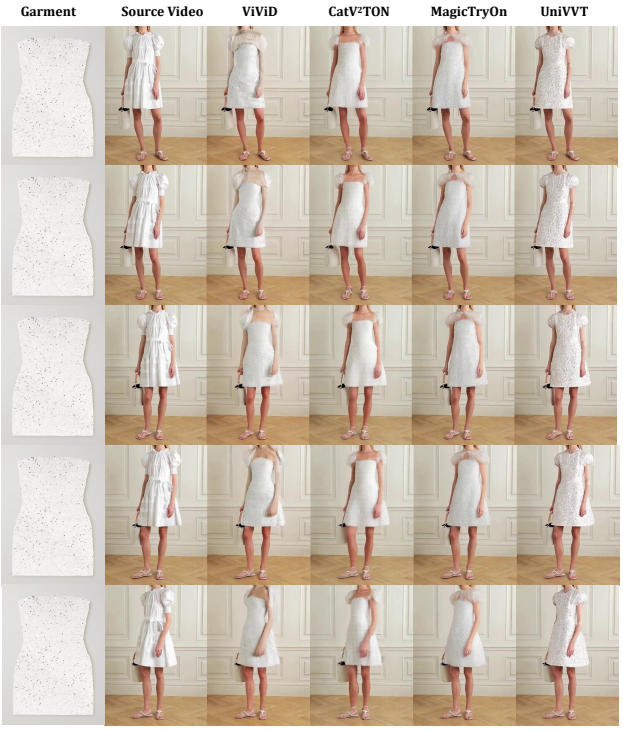


Figure 14: Subtle texture preservation in video try-on.

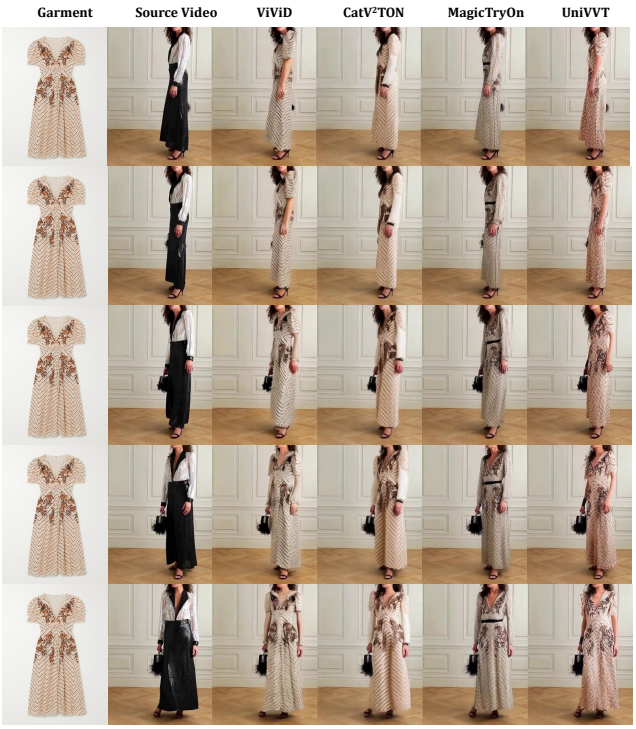


Figure 15: Pattern and color fidelity in video try-on.



Figure 16: Complete trouser replacement in video try-on.



Figure 17: Source-garment leakage suppression in video try-on.

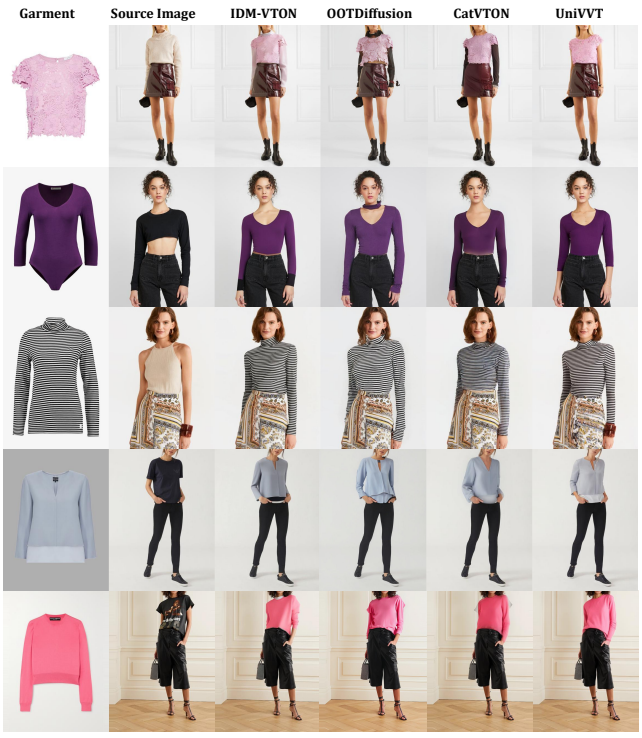


Figure 18: Upper-body image try-on comparison.



Figure 19: Lower-body image try-on comparison.



Figure 20: Dress image try-on comparison.



Figure 21: Cross-category failure cases with ambiguous editing extent. Replacing a dress with an upper-body garment requires determining which previously covered regions should be preserved, removed, or synthesized; none of the evaluated methods resolves this ambiguity reliably.